Comparative Medicine
Copyright 2013
by the American Association for Laboratory Animal Science

Vol 63, No 5
October 2013
Pages 448–453

Case Report

Metastatic Hepatocellular Carcinoma in a Juvenile Rhesus Macaque (*Macaca mulatta*)

Steven T Laing, Marie J Lemoy,* Rebecca L Sammak, and Ross P Tarara

Neoplasia in juvenile (younger than 5 y) rhesus macaques has been estimated to represent only approximately 1.4% of all occurrences of spontaneous neoplasia. Here we report an unusual case of a 3.75-y-old primiparous female rhesus macaque that was euthanized due to poor prognosis associated with progressive anemia, marked hepatomegaly, and radiographic evidence of metastatic neoplasia. Postmortem examination revealed an invasive, hemorrhagic hepatic mass that effaced approximately 70% of the liver parenchyma and had evidence of metastatic spread to multiple abdominal organs, the lungs, and the pituitary gland. Neoplastic polygonal cells lined large necrohemorrhagic cavities and exhibited marked anisocytosis and anisokaryosis, with frequent multinucleate cells. There was no desmoplasia associated with the primary neoplasm or metastases. Immunohistochemical studies revealed the neoplastic cells to be diffusely reactive with pancytokeratin, cytokeratin 7, and cytokeratin 8/18 antibodies and rarely reactive with carcinoembryonic antigen antibodies. The cells did not react with vimentin, S100, CD31, or factor VIII antibodies. Tumor morphology and immunophenotype led to the diagnosis of anaplastic hepatocellular carcinoma. This report represents the first known case of metastatic liver neoplasia in a rhesus macaque. The young age of this animal and the aggressive nature of the neoplasm are highly unusual and reminiscent of adolescent onset hepatocellular carcinoma in humans.

Abbreviations: CK, cytokeratin; HCC, Hepatocellular carcinoma.

Neoplasia in juvenile rhesus macaques (*Macaca mulatta*) is extremely uncommon.[17,18] In a recent review of spontaneous neoplasia in 2 colonies of rhesus macaques, animals younger than 5 y represented only 1.4% of the total number of cases, and primary hepatic tumors were uncommon.[18] All 5 of the cases detected among 2660 macaques involved animals between 14 and 26.8 y of age, and none had evidence of metastasis. Primary hepatic tumors appear to be similarly infrequent occurrences in other nonhuman primates, with the notable exception of prosimians, in which tumors arising from the liver are common spontaneous neoplasms.[3,15,17,18] Malignant liver tumors account for only 1% of pediatric tumors in humans.[5,7,12] Approximately 80% of these are hepatoblastomas—neoplasms arising from liver progenitor cells—and hepatocellular carcinoma (HCC) represents the second most frequent diagnosis.[5,7,12]

The medicine department of the California National Primate Research Center evaluated a 3.75-y-old, sexually mature, female rhesus macaque for rapidly progressive disease associated with a hepatic mass. Anaplastic HCC with extensive metastasis was diagnosed after postmortem examination. The current report describes the clinical progression of disease, the gross and microscopic pathology of the affected macaque, and the immunohistochemical characterization of the neoplasm.

Received: 15 Jan 2013. Revision requested: 05 Mar 2013. Accepted: 15 Apr 2013.
California National Primate Research Center, University of California at Davis, Davis, California.
**Corresponding author. Email: mjlemoy@primate.ucdavis.edu*

Case Report

Clinical findings. A 3.75-y-old, 6.0-kg female rhesus macaque was presented to the hospital in March 2012 for an abdominal mass that was palpated during a routine, semiannual physical exam. The animal was bred and maintained at the California National Primate Research Center, an AAALAC-accredited facility, in a large conventional outdoor breeding colony in accordance with the Animal Welfare Act and the *Guide for the Care and Use of Laboratory Animals*.[1,8] Protocols for maintenance and breeding of rhesus macaque colonies were approved by the University of California Davis IACUC. The macaque had not undergone any experimental procedures or manipulations prior to her presentation and had no pertinent previous medical history.

On initial presentation, the macaque was active and was caring for a 5-d-old infant. She was sedated with ketamine (12 mg/kg IM, Butler Animal Health Supply, Dublin, OH) to facilitate performance of a complete physical exam, whole-blood analysis (Nova-CCX Stat Analyzer, Nova Biomedical, Waltham, MA), hematology, serum biochemistry profile, abdominal radiography, and abdominal ultrasonography. Clinical examination under sedation revealed the presence of a grossly enlarged liver that extended approximately 5 cm beyond the costal arch, occupying about half of the abdominal cavity. The macaque's temperature, heart rate, and respiratory rate were within normal limits. Palpation revealed the presence of a small involuting uterus, considered to be normal for a macaque at 5 d postpartum.

At initial presentation, the macaque demonstrated a mild normocytic, hypochromic anemia with polychromasia (Table 1), interpreted as a regenerative hemogram. Moderately elevated

Table 1. CBC counts of the affected juvenile rhesus macaque on days 1 and 14 after presentation

	Day 1	Day 14	Reference range[a]
Hct (%)	25.6	20.9	38.3–42.3
Hgb (g/dL)	7.7	5.9	12.2–13.4
MCV (fL)	68	68	67.0–73.0
MCH (pg)	20.3	19.3	21.2–23.2
MCHC (pg/fL)	30	28.3	31.0–32.4
Platelets (x10^5/μL)	2.23	1.97	3.56–6.54
No. of nucleated RBC per 100 WBC	2	18	0
WBC (x10^3/μL)	12.5	15.2	6.4–10.2
Band neutrophils	0	5	0.0–1.0
Neutrophils (x10^3/μL)	10.5	9.27	1.93–9.28
Lymphocytes (x10^3/μL)	1.25	5.17	1.59–7.33
Monocytes (x10^3/μL)	0.75	0	0–0.27
Fibrinogen (mg/dL)	400	294	100–300

[a]From reference 17.

fibrinogen and mild neutrophilia were consistent with an inflammatory process. Evidence of ongoing hepatocellular damage and cholestasis was provided by moderately elevated serum ALT (161 U/L; reference range, 26 to 52 U/L), AST (189 U/L; reference range, 24 to 38 U/L), LDH (4830 U/L; reference range, 217 to 419 U/L), ALP (674 U/L; reference range, 46 to 256 U/L), and GGT (140 U/L; reference range, 48 to 76 U/L).[19] In addition, moderately decreased serum albumin (2.1 g/dL; reference range, 4.1 to 4.7 g/dL), mildly decreased cholesterol (83 mg/dL; reference range, 148 to 200), slightly elevated BUN (33 mg/dL; reference range, 16 to 22 mg/dL), and normal total bilirubin (0.3 mg/dL; reference range 0.1 to 03 mg/dL) were present.[19]

Abdominal radiographs and ultrasonograms confirmed the presence of severe hepatomegaly. On abdominal radiographs, the caudoventral liver margins had decreased serosal detail and extended beyond the costal arch, with displacement of the gastric axis. Ultrasonography revealed multiple nodules of mixed echogenicity that extended throughout the liver parenchyma, disrupted normal architecture, and resulted in rounded, undulating liver margins (Figure 1 A). There was a moderate amount of free abdominal fluid between liver lobes and elsewhere in the abdomen. Fluid samples obtained by abdominocentesis were consistent with hemorrhage.

The next day, the macaque again was sedated with ketamine (10 mg/kg), and blood samples were drawn for hepatitis A and B serology, PT, and PTT time. Hepatitis A serology was consistent with historical exposure but not current infection (combined IgG and IgM, reactive; IgM, nonreactive). Tests for hepatitis B surface antigen and antibody were negative. PT was within normal limits (13.4 s; reference range, 9.4 to 13.9 s), and PTT was mildly prolonged (29.7 s; reference range, 18.6 to 24.7 s).[19]

Five days after the initial presentation, an ultrasound-guided percutaneous biopsy of the macaque's liver was performed under ketamine (10 mg/kg, IM) and dexmedetomidine (0.03 mg/kg IM; Pfizer Animal Health, New York, NY) sedation. Sedation was reversed with atipemazole (0.15 mg/kg IM; Pfizer Animal Health). Ultrasound examination at this time revealed increased parenchymal disruption and multiple hypoechoic regions within the liver. Biopsy samples were obtained (18-gauge EZ Core Single-action Biopsy Needle, Products Group International, Lyons, CO) from 2 hepatic nodules and submitted in 10% phosphate-buffered formalin for histopathologic examination. When examined, the biopsy tissue sample revealed extensive necrosis, with only rare peripheral, large polygonal cells with vesicular nuclei. As such the sample was considered to be nondiagnostic.

Despite the severity of the macaque's disease, she consistently had a good appetite and continued to provide good maternal care to her infant. At 14 d after initial presentation, the animal was reassessed under ketamine sedation (10 mg/kg), whereupon the liver had increased dramatically in size, extending approximately 10 cm beyond the costal arch, and her mucous membranes appeared pale. A CBC count was repeated; revealing a worsening anemia, increased nucleated RBC count, and increased leukocytosis (Table 1). Abdominal ultrasonography and abdominal and thoracic radiography showed substantial enlargement of the liver and multiple small, round, soft-tissue-opacity nodules throughout the lung fields (Figure 1 B and C).

Due to the grave prognosis and rate of disease progression, the macaque was euthanized by using pentobarbital (0.25 g/kg IV; Vortech Pharmaceuticals, Dearborn, MI) and submitted for complete necropsy. The infant was maintained temporarily in a nursery until a foster dam was identified.

Pathology. The macaque was presented to necropsy in fair nutritional condition, weighing 5.46 kg, and with a markedly swollen abdomen. The peritoneal cavity contained approximately 20 to 30 mL of serosanguinous fluid. The liver was markedly enlarged, with multiple adhesions between it, the diaphragm, right kidney, and omentum. The liver weighed 705.8 g (12.9% of body weight). It had a highly irregular, multinodular surface that was mottled dark red, purple, and tan (Figure 2 A). Individual nodules were soft, friable, as large as 3.0 cm in diameter, and multifocally umbilicated. The nodules were confluent throughout the liver parenchyma and, on cut section, frequently were cavitated and contained gelatinous, clotted blood or pale tan, friable, necrotic material (Figure 2 B). Multiple similar dark-red and tan masses expanded and disrupted the parenchyma of the hepatopancreatic, mesenteric, and paravertebral lymph nodes; the pancreas; the left adrenal gland; and both kidneys (Figure 2 C). An additional 3 similar masses expanded the splenic parenchyma. The largest of these masses measured 2.5 cm × 2.3 cm × 1.9 cm, and a small amount of dark red, gelatinous tissue protruded through the capsule (hemorrhage). The lungs contained 30 to 60 dark-red to tan, firm, and frequently umbilicated nodules that measured as large as 0.9 cm in diameter and were scattered throughout all lung lobes (Figure 2 D). Interestingly, the pituitary gland contained a single similar nodule, but there was no evidence of extension to the brain. Representative sections of liver, spleen, kidneys, urinary bladder, pancreas, adrenal glands, thyroid glands, gastrointestinal tract, reproductive tract, heart, trachea, lung, visceral and peripheral lymph nodes, pituitary gland, and brain were submitted in 10% phosphate-buffered formalin, embedded in paraffin, cut at 5 μm, and stained with hematoxylin and eosin.

Approximately 60% to 70% of the examined sections of liver were replaced by coalescing blood-filled, necrotic cavities that were discontinuously lined by round to polygonal neoplastic cells and separated by bands of compressed hepatic parenchyma without a surrounding desmoplastic response (Figure 3 A). The

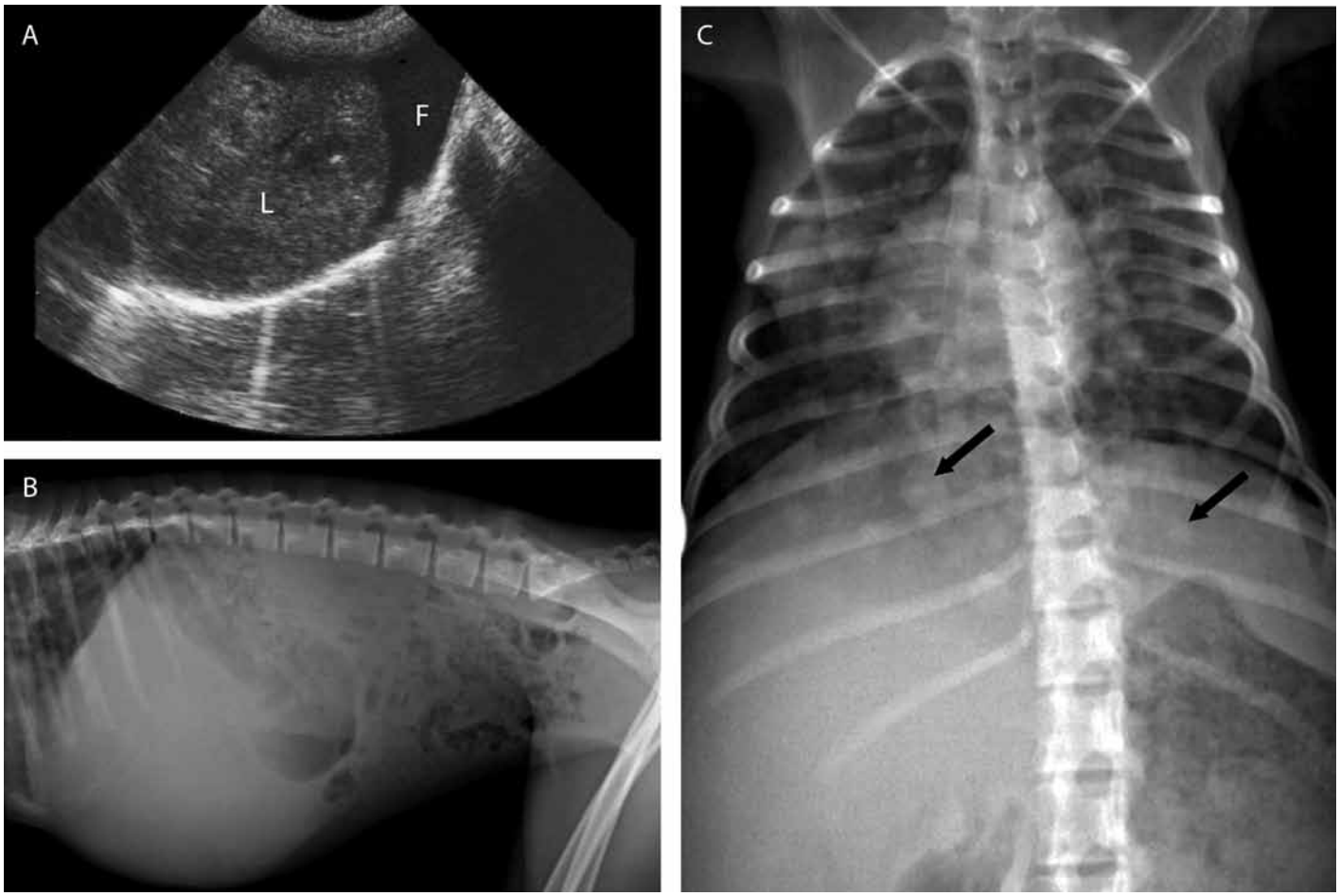

Figure 1. (A) Ultrasonogram, day of presentation. The liver (L) is enlarged, with an undulating margin and multiple hypoechoic regions. There is free fluid (F) in the abdomen. (B) Right lateral abdominal radiograph, 14 d after presentation. The liver is markedly enlarged and distends the abdominal cavity. (C) Anterior–posterior thoracic radiograph, 14 d after presentation. Multiple round soft-tissue opacities (arrows) are scattered throughout all lobes of the lungs.

neoplastic cells had a variably high nuclear-to-cytoplasmic ratio, with a small amount of microvesicular, pale amphophilic cytoplasm. The cells were arranged in sheets, multifocally supported by a fine fibrovascular stroma. Nuclei were central, round to oval, and had 1 to 3 magenta nucleoli. There was marked anisokaryosis and anisocytosis, with frequent multinucleate giant neoplastic cells (Figure 3 A). Mitotic figures were bizarre and frequent, averaging more than 4 per 400× field. The masses and nodules noted in multiple other organs were composed of the same neoplastic cells, and most were similarly necrotic and hemorrhagic (Figure 3 B). Given the extensive involvement of the liver and the metastatic pattern of spread in other organs, a primary hepatic tumor was suspected, which prompted immunohistochemical studies.

Immunohistochemistry. Immunohistochemistry was performed on 4-µm-thick, formalin-fixed, paraffin-embedded tissue sections, mounted on charged slides and air-dried overnight at 37 °C. Sections were rehydrated through xylene and 95% and 70% reagent alcohols to PBS (pH 7.4). Sections were quenched with 0.3% hydrogen peroxide in methanol prior to rehydration with 70% alcohol. Antigen retrieval was accomplished by using either heat-induced epitope retrieval with target retrieval solution (S1699, Dako North America, Carpinteria, CA) for 30 min at 95 °C and a 20-min cool down or by using enzymatic digestion with proteinase K (S3020, Dako North America) according to the manufacturer's instructions. The antibody and blocking diluents and all subsequent rinses were 0.02% Tween-20 in PBS. Sections were blocked for 20 min in 10% normal horse serum. All incubations were performed in a humidified chamber at room temperature.

Primary antibody type, dilution, and antigen retrieval were as follows: mouse antipancytokeratin (CK; clone LU5; CM043C, Biocare Medical, Concord, CA), 1:100, heat-induced epitope retrieval; mouse antivimentin (clone 3B4; M7020, Dako North America), 1:300, enzymatic digestion for 7 min; rabbit antiS100 Protein R (VP-S276, Vector Laboratories, Burlingame, CA), 1:400, heat-induced epitope retrieval; rabbit antifactor VIII (A0082, Dako North America), 1:2000, enzymatic digestion for 10 min; mouse antiCD31 (clone JC70A; M0823, Dako North America), 1:50, heat-induced epitope retrieval; mouse antiCK 8/18 (clone Zym5.2, UCD/PR-10.11; 18-0213, Zymed, San Francisco, CA), 1:250, enzymatic digestion for 7 min; mouse antiCK 7 (clone OV-TL 12/30; MU255-UC, BioGenex, Fremont, CA), 1:100, enzymatic digestion for 10 min; and rabbit anticarcinoembryonic

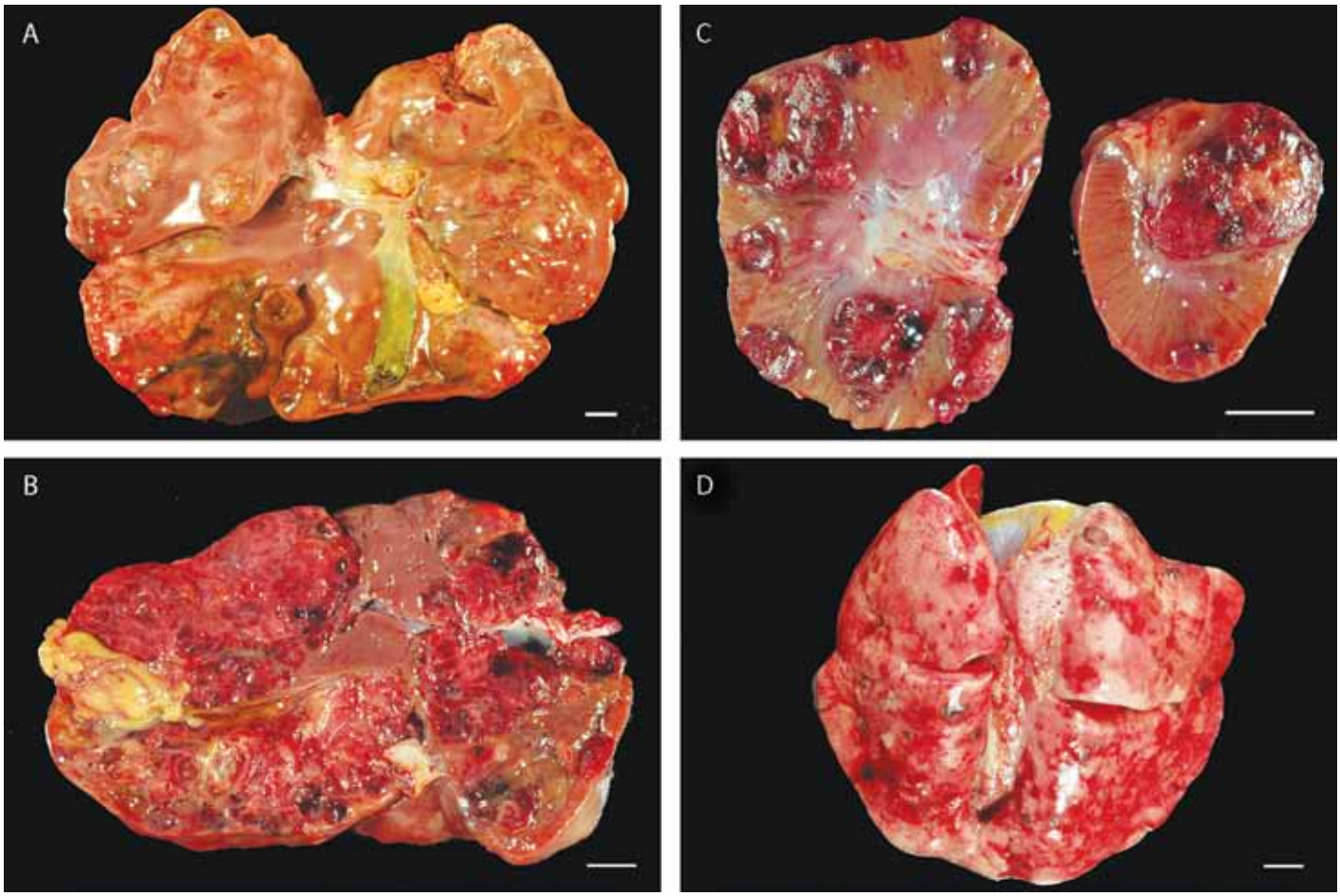

Figure 2. (A) Multiple coalescing nodules markedly enlarge all lobes of the liver. (B) On cut section, the nodules are hemorrhagic and replace approximately 60% to 70% of the normal hepatic parenchyma. (C) Multiple hemorrhagic nodules are scattered throughout all lobes of the lungs. (D) Similar nodules are scattered throughout the kidneys. Bar, 1 cm.

antigen (A0115, Dako North America), 1:200, heat-induced epitope retrieval. Primary antibodies to CK7 and carcinoembryonic antigen were detected by using peroxidase-conjugated antimouse or antirabbit antibodies, respectively (K4001 and K003, Dako North America) for 30 min. Primary antibodies to CD31, factor VIII, CK8/18, vimentin, panCK, and S100 were detected by using a 2-step horseradish peroxidase and alkaline phosphatase method (HM606, GR608, and HP604, respectively, Biocare Medical) for 10 min each reagent. Rinses (3 min each) occurred twice between each reagent application. Detection was visualized by using a peroxidase substrate kit (SK4800, Vector Laboratories) according to the manufacturer's instructions. Sections were counterstained in Mayer hematoxylin, air-dried, and coverslipped. Nonspecific background was evaluated by using duplicate sections processed by using heat-induced epitope retrieval, diluent in place of the primary antibody, and detection with the antimouse linker.

PanCK, vimentin, and S100 antibodies were applied initially to sections of affected liver, adrenal gland, and pituitary gland. In all of these sections, the cytoplasm of the neoplastic cells was reactive with pancytokeratin antibody but did not react with vimentin or S100 antibodies. However, vimentin immunohistochemistry highlighted the dense network of thin-walled vessels associated with the neoplasm. CK8/18, which is expressed in the cytoplasm of mature hepatocytes and cholangiocytes;[16] CK7, which is expressed in the cytoplasm of cholangiocytes and progenitor cells of the canals of Hering;[16] carcinoembryonic antigen, which is expressed in the canaliculi of hepatocytes;[16] and CD31 and factor VIII, both markers of endothelial cells,[22] were applied to only the affected liver. There was strong cytoplasmic reactivity to both CK8/18 and CK7 antibodies (Figure 4). Rare neoplastic cells, and particularly multinucleate variants, had weak, granular cytoplasmic reactivity with antibody to carcinoembryonic antigen (Figure 4). Neoplastic cells did not react with CD31 and factor VIII antibodies. Combined with the tumor morphology, these results supported the final diagnosis of anaplastic HCC.

Discussion

This report represents the first known case of naturally occurring metastatic liver neoplasia in a rhesus macaque. A recent review of spontaneous neoplasia in rhesus macaques over more than 20 y reported one case of HCC (in a 14-y-old macaque) and one case of anaplastic HCC (in a 20.5-y-old macaque).[18] Neither animal had evidence of metastasis.[18]

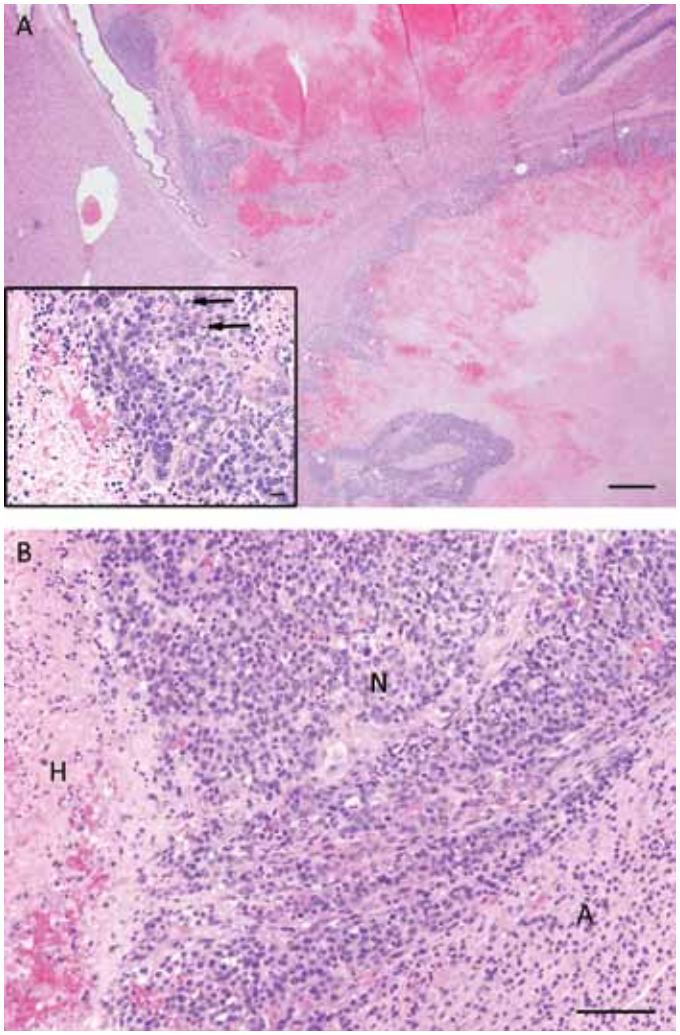

Figure 3. (A) Large regions of the liver are replaced by hemorrhagic and necrotic material lined by dense sheets of neoplastic polygonal cells. Hematoxylin and eosin stain; bar, 500 µm. Inset, Neoplastic cells are highly pleomorphic, with many multinucleate cells and numerous mitotic figures (arrows). Hematoxylin and eosin stain; bar, 20 µm. (B) The tumor metastases in the adrenal gland have a similar morphology to that of the primary mass. Densely packed neoplastic cells (n) infiltrate and compress the adjacent adrenal cortex (a). There are large regions of hemorrhage and necrosis (h). Hematoxylin and eosin stain; bar, 100 µm.

Other studies have found spontaneous malignant hepatic neoplasia, including HCC and cholangiocarcinomas, to be extremely uncommon in macaques and rare in other Old World nonhuman primates.[3,17,20] However, sporadic cases of hepatic neoplasia have been reported to occur in a capuchin monkey (*Cebus albifrons*),[2] a squirrel monkey (*Saimiri sciureus*),[13] and 2 juvenile cynomolgus macaques (*Macaca fascicularis*).[14] Both affected cynomolgus macaques were male and younger than 5 y. According to tumor morphology and a panel of immunohistochemical markers, one animal was diagnosed with a solitary HCC, and the other had multiple intrahepatic HCC and a mixed hepatocholangiocellular carcinoma. Neither had evidence of extrahepatic metastasis.[14]

Despite the fact that an estimated 70% of our rhesus macaque's liver was effaced, biochemical parameters, including a coagulation panel, did not support decreased hepatic function. This finding highlights the remarkable reserve capacity of the liver and is consistent with the paradigm that 80% to 90% of hepatic mass must be lost before function is affected.[4] The cause of this animal's progressive anemia was likely chronic ongoing hemorrhage associated with the tumors. Indeed, the hemorrhagic appearance of the masses was at first confusing, and hemangiosarcoma was considered as a diagnosis in light of the gross pathology. However, the neoplastic cells were diffusely immunoreactive with CK7 and CK8/18 antibodies, rarely reactive with antibodies to carcinoembryonic antigen, and did not react with vimentin, CD31, or factor VIII antibodies. These results are inconsistent with a mesenchymal or endothelial histogenesis.

In normal liver, CK7 expression is restricted to bile duct epithelium, as we saw in regions of unaffected liver in this case, and the progenitor cells of the canals of Hering.[16] However, in humans, some HCCs have been shown to express CK7 in addition to CK8/18.[16] CK19, another keratin that is restricted to the bile ducts and progenitor cells in normal liver, may also be expressed by HCC.[16,21] Expression of these keratins is thought to point to a common hepatic progenitor cell that gives rise to both hepatocytes and cholangiocytes. HCC and cholangiocarcinoma are now thought to represent a spectrum of neoplasms with a similar histogenesis.[16] The differential diagnoses in the case we present were hepatoblastoma, in light of the young age of the affected animal, cholangiocarcinoma, and HCC. These tumors may all have similar immunophenotypes. We consider anaplastic HCC to be the most appropriate diagnosis, given the lack of small, blue embryonal cells and a mesenchymal component within the neoplasm, which characteristics may be expected in hepatoblastomas.[5] The lack of ductular structures and scirrhous response made cholangiocarcinoma an unlikely diagnosis.[9] In addition, hepatoblastomas in humans typically present as large solitary masses in the right lobe of the liver, unlike the diffuse replacement of the hepatic parenchyma in our case.[12] Interestingly, human HCC that are immunoreactive with both CK8/18 and CK7, similar to the findings in the current study, have been shown to have a worse prognosis than those that are CK7-negative.[21]

HCC in human children and adults frequently is associated with infectious or noninfectious chronic inflammatory disease.[7] In particular, perinatal transmission of hepatitis B virus is associated with HCC in young children. The advent of vaccination protocols has significantly reduced the incidence of hepatitis-B–associated HCC[12] However, HCC also presents a second peak of incidence in adolescents, when it is not associated with prior inflammation and has an extremely poor prognosis.[7,12] Natural hepatitis B infections are rare in macaques, having been reported in only 2 cynomolgus macaques.[10] Hepatitis-B-associated carcinogenesis has only been produced experimentally after simultaneous exposure to diethylnitrosamine.[6] In addition, chronic experimental exposure of macaques to several other carcinogens, including aflatoxin B1, has been shown to result in hepatic malignancies.[20] The macaque we describe here was serologically negative for hepatitis B and had no evidence of ongoing hepatitis A infection. Hepatitis A infection typically results in mild, subclinical hepatitis and has not been associated with the development of HCC.[11] Our macaque was not enrolled in any experimental protocols and had no known exposure to toxins. Therefore, the clinical

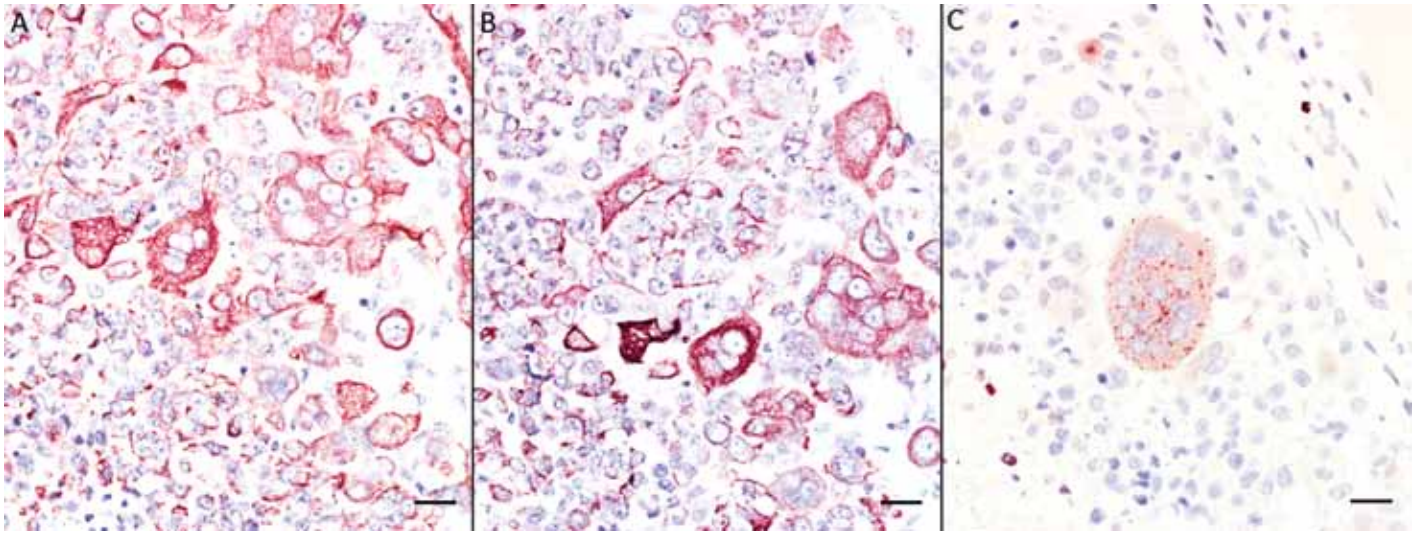

Figure 4. Neoplastic cells in the liver exhibit strong cytoplasmic reaction with (A) CK8/18 and (B) CK7 antibodies. (C) Rare multinucleate neoplastic cells exhibit granular cytoplasmic reaction with antibodies to carcinoembryonic antigen. Immunohistochemistry; bar, 20 µm.

history and signalment of our macaque is most similar to that of human adolescents with HCC.

Acknowledgment

We acknowledge the expertise of Michael Manzer, who performed the immunohistochemistry described in this report.

References

1. **Animal Welfare Act as Amended.** 2008. 7 USC §2131–2159.
2. **Brown RJ, O'Neill TP, Kessler MJ, Andress D.** 1980. Cholangiocarcinoma in a capuchin monkey (*Cebus albifrons*). Vet Pathol **17:**626–629.
3. **Cianciolo RE, Butler SD, Eggers JS, Dick EJ Jr, Leland MM, de la Garza M, Brasky KM, Cummins LB, Hubbard GB.** 2007. Spontaneous neoplasia in the baboon (*Papio* spp.). J Med Primatol **36:**61–79.
4. **Crawford JM, Liu C.** 2010. Liver and biliary tract, p 833–890. In: Kumar V, Abbas AK, Fausto N, Aster JC, editors. Robbins and Cotran pathologic basis of disease. Philadelphia (PA): Saunders/ Elsevier.
5. **Finegold MJ, Egler RA, Goss JA, Guillerman RP, Karpen SJ, Krishnamurthy R, O'Mahony CA.** 2008. Liver tumors: pediatric population. Liver Transpl **14:**1545–1556.
6. **Gyorkey F, Melnick JL, Mirkovic R, Cabral GA, Gyorkey P, Hollinger FB.** 1977. Experimental carcinoma of liver in macaque monkeys exposed to diethylnitrosamine and hepatitis B virus. J Natl Cancer Inst **59:**1451–1467.
7. **Hadzic N, Finegold MJ.** 2011. Liver neoplasia in children. Clin Liver Dis **15:**443–462.
8. **Institute for Laboratory Animal Research.** 2011. Guide for the care and use of laboratory animals, 8th ed. Washington (DC): National Academies Press.
9. **Kajiyama K, Maeda T, Takenaka K, Sugimachi K, Tsuneyoshi M.** 1999. The significance of stromal desmoplasia in intrahepatic cholangiocarcinoma: a special reference of 'scirrhous-type' and 'nonscirrhous-type' growth. Am J Surg Pathol **23:**892–902.
10. **Kornegay RW, Giddens WE Jr, Van Hoosier GL Jr, Morton WR.** 1985. Subacute nonsuppurative hepatitis associated with hepatitis B virus infection in 2 cynomolgus monkeys. Lab Anim Sci **35:**400–404.
11. **Lankas GR, Jensen RD.** 1987. Evidence of hepatitis A infection in immature rhesus monkeys. Vet Pathol **24:**340–344.
12. **Litten JB, Tomlinson GE.** 2008. Liver tumors in children. Oncologist **13:**812–820.
13. **Morris TH, Abdi MM.** 1996. Hepatocellular carcinoma in a squirrel monkey (*Saimiri sciureus*). J Med Primatol **25:**137–139.
14. **Reindel JF, Walsh KM, Toy KA, Bobrowski WF.** 2000. Spontaneously occurring hepatocellular neoplasia in adolescent cynomolgus monkeys (*Macaca fascicularis*). Vet Pathol **37:**656–662.
15. **Remick AK, Van Wettere AJ, Williams CV.** 2009. Neoplasia in prosimians: case series from a captive prosimian population and literature review. Vet Pathol **46:**746–772.
16. **Roskams T.** 2011. Anatomic pathology of hepatocellular carcinoma: impact on prognosis and response to therapy. Clin Liver Dis **15:**245–259.
17. **Seibold HR, Wolf RH.** 1973. Neoplasms and proliferative lesions in 1065 nonhuman primate necropsies. Lab Anim Sci **23:**533–539.
18. **Simmons HA, Mattison JA.** 2011. The incidence of spontaneous neoplasia in 2 populations of captive rhesus macaques (*Macaca mulatta*). Antioxid Redox Signal **14:**221–227.
19. **Summers L.** 2011. Veterinary pharmaceutical formulary and clinical reference handbook. Davis (CA): Regents of the University of California.
20. **Thorgeirsson UP, Dalgard DW, Reeves J, Adamson RH.** 1994. Tumor incidence in a chemical carcinogenesis study of nonhuman primates. Regul Toxicol Pharmacol **19:**130–151.
21. **Uenishi T, Kubo S, Yamamoto T, Shuto T, Ogawa M, Tanaka H, Tanaka S, Kaneda K, Hirohashi K.** 2003. Cytokeratin 19 expression in hepatocellular carcinoma predicts early postoperative recurrence. Cancer Sci **94:**851–857.
22. **Wick MR, Hornick JL.** 2010. Immunohistology of soft tissue and osseous neoplasms, p 83–136. In: Dabbs DJ, editor. Diagnostic Immunohistochemistry. Philadelphia (PA): Saunders.